JCB Article

MAL regulates clathrin-mediated endocytosis at the apical surface of Madin–Darby canine kidney cells

Fernando Martín-Belmonte,[1] José A. Martínez-Menárguez,[2] Juan F. Aranda,[1] José Ballesta,[2] María C. de Marco,[1] and Miguel A. Alonso[1]

[1]Centro de Biología Molecular "Severo Ochoa", Universidad Autónoma de Madrid and Consejo Superior de Investigaciones Científicas, Cantoblanco, Madrid, 28049 Spain
[2]Departamento de Biología Celular, Facultad de Medicina, Universidad de Murcia, Murcia, 30071 Spain

MAL is an integral protein component of the machinery for apical transport in epithelial Madin–Darby canine kidney (MDCK) cells. To maintain its distribution, MAL cycles continuously between the plasma membrane and the Golgi complex. The clathrin-mediated route for apical internalization is known to differ from that at the basolateral surface. Herein, we report that MAL depends on the clathrin pathway for apical internalization. Apically internalized polymeric Ig receptor (pIgR), which uses clathrin for endocytosis, colocalized with internalized MAL in the same apical vesicles. Time-lapse confocal microscopic analysis revealed cotransport of pIgR and MAL in the same endocytic structures. Immunoelectron microscopic analysis evidenced colabeling of MAL with apically labeled pIgR in pits and clathrin-coated vesicles. Apical internalization of pIgR was abrogated in cells with reduced levels of MAL, whereas this did not occur either with its basolateral entry or the apical internalization of glycosylphosphatidylinositol-anchored proteins, which does not involve clathrin. Therefore, MAL is critical for efficient clathrin-mediated endocytosis at the apical surface in MDCK cells.

Introduction

In polarized epithelial cells, the composition of the apical and basolateral membrane subdomains is maintained by specialized exocytic and endocytic pathways that sort newly synthesized and internalized proteins, respectively, specifically to each surface subdomain (Mostov et al., 2000). Clathrin-mediated endocytosis takes place at both the apical and basolateral domains but the process differs at both membrane surfaces (Naim et al., 1995). The mechanisms of exocytic transport are also different for each membrane surface (Matter and Mellman, 1994). In epithelial MDCK cells, sorting to the basolateral surface is mediated by sequences in the cytoplasmic tail of membrane proteins that might or might not be related to tyrosine- and dileucine-based sorting signals (Mellman et al., 1993). In contrast, a direct pathway of transport to the apical membrane appears to be mediated by integration of cargo proteins into specialized glycolipid-enriched membrane microdomains or rafts (Simons and Wandinger-Ness, 1990).

MAL is a raft-associated integral membrane protein of 17 kD, which has been demonstrated to be an essential element of the machinery for efficient apical transport in MDCK cells (Cheong et al., 1999; Puertollano et al., 1999; Martin-Belmonte et al., 2000, 2001). Despite the intense vesicular traffic to deliver newly synthesized apical cargo, MAL accumulation at the plasma membrane is prevented by continuous recycling to the Golgi complex via the endosomal system, which, in addition, allows its participation in new rounds of cargo transport (Puertollano and Alonso, 1999). At steady state, ~12% of MAL is detected in the plasma membrane including clathrin-coated pits and buds in MDCK cells (Puertollano et al., 2001). Here, we have analyzed the clathrin requirement for MAL internalization and investigated the role of MAL in the internalization of apical proteins. As model proteins, we used the polymeric Ig receptor (pIgR) and the transferrin receptor, which are known to internalize from both the apical and basolateral surface

The online version of this article contains supplemental material.

Address correspondence to Miguel A. Alonso, Centro de Biología Molecular "Severo Ochoa", Universidad Autónoma de Madrid and Consejo Superior de Investigaciones Científicas, Cantoblanco, Madrid, 28049 Spain. Tel.: 34-91-397-8037. Fax: 34-91-397-8087. email: maalonso@cbm.uam.es

Key words: apical endocytosis; protein machinery; polarized transport; epithelial cells; lipid rafts

Abbreviations used in this paper: FR, folate receptor; GPI, glycosylphosphatidylinositol; NHS-SS-biotin, sulfosuccinimidyl 2-(6-(biotinamido)hexanoamido)ethyl-1-3′-dithiopropionate; pIgR, polymeric Ig receptor; sulfo-NHS-biotin, sulfo-*N*-hydroxyl-succinimido-biotin.

through a clathrin-mediated pathway (Odorizzi et al., 1996; Altschuler et al., 1999), and glycosylphosphatidylinositol (GPI)-anchored proteins, such as placental alkaline phosphatase and folate receptor (FR), which use clathrin-independent mechanisms (Nichols and Lippincott-Schwartz, 2001). Our results indicate that MAL uses clathrin for apical endocytosis and that MAL is required for internalization of pIgR and transferrin receptor from the apical, but not from the basolateral, surface or apical endocytosis of GPI-anchored proteins.

Results

Apical endocytosis of MAL takes place by a clathrin-dependent pathway in MDCK cells

To detect MAL on the cell surface and to track its internalization, we prepared stable transfectants of MDCK cells (MDCK/MAL-FLAG cells) that stably expressed a MAL protein bearing a FLAG tag in its last extracellular/luminal loop (MAL-FLAG). The tag makes MAL-FLAG accessible to anti-FLAG antibodies from the extracellular space (Puertollano and Alonso, 1999). To interfere with clathrin-mediated endocytosis, we transiently expressed GFP-DPF coil, an EH-deleted form of the Eps 15 protein tagged with the GFP, which behaves as a dominant-negative mutant and provokes a block of clathrin-coated pit endocytosis (Benmerah et al., 1999). MDCK/MAL-FLAG cells were transfected with GFP-DPF coil, plated, and left to polarize for 48 h in tissue culture filter inserts. The transepithelial resistance of the cell monolayer was measured to ensure proper tight junction formation. As a control for cell polarization, the distributions of gp135 and E-cadherin, chosen as apical and basolateral markers, respectively, were determined in parallel cultures. Fig. 1 A shows that, consistent with the presence of MAL in surface clathrin pits and buds (Puertollano et al., 2001), overexpression of GFP-DPF coil led to a complete block of MAL-FLAG apical internalization. As controls, we observed in parallel that overexpression of

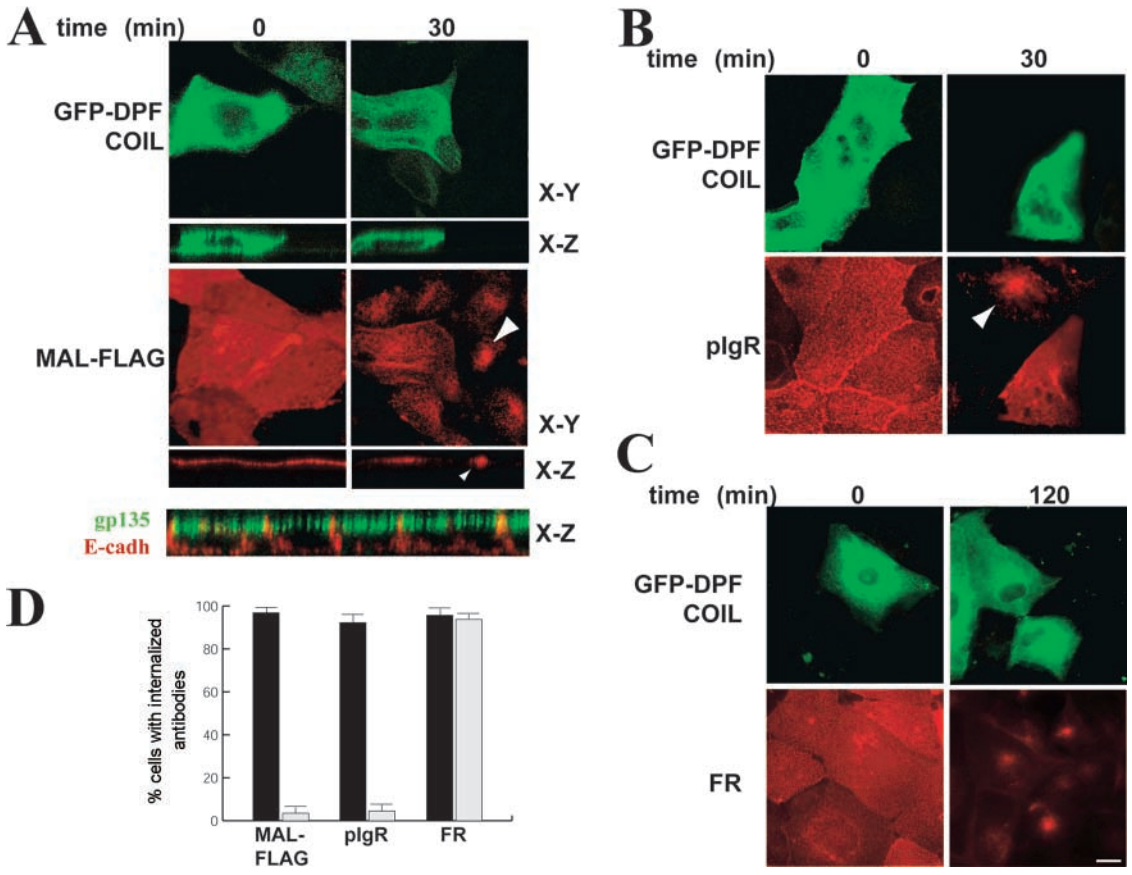

Figure 1. **Effect of a dominant-negative mutant of Eps15 on apical internalization of MAL.** MDCK/MAL-FLAG, MDCK/pIgR or MDCK/FR cells, which stably express MAL-FLAG, pIgR and FR, respectively, were transiently transfected with GFP-DPF coil cDNA. The cells were plated onto tissue culture filters and left to polarize for 48 h at 37°C. Cells were incubated with (A) Alexa-594–labeled anti-FLAG, (B) anti-pIgR, or (C) anti-FR antibodies from the apical surface at 4°C for 30 min, washed, and fixed (time 0) or shifted to 37°C for 30 min to allow internalization before fixation. Cells were then analyzed by confocal immunofluorescence microscopy. Optical x-y and x-z sections are presented in A, whereas only x-y sections are shown in B and C. As an internal control, internalization of MAL-FLAG and pIgR was observed in cells not expressing GFP-DPF coil (arrowheads). MAL-FLAG internalization in the absence of GFP-DPF coil is clearly detected in the corresponding x-z view (arrowhead). FR internalized regardless of the expression of GFP-DPF coil. Note that, although the cell monolayer was tightly confluent, only the cells expressing the exogenous products are stained. As a control of polarization, the cell monolayers were stained after fixation and permeabilization for gp135 and E-cadherin, as markers for the apical and basolateral surface, respectively. Bar, 10 μm. (D) The percentage of untransfected (black bars) and GFP-DPF coil-transfected (gray bars) cells with internalized MAL-FLAG, pIgR or FR is shown. The values shown are the mean of three independent replicates. Greater than 100 cells from each case were analyzed.

GFP-DPF coil halted the apical internalization of pIgR (Fig. 1 B) but did not affect that of FR (Fig. 1 C) in MDCK/pIgR and MDCK/FR cells that stably express pIgR and FR, respectively. Quantitative analysis showed that the great majority of cells positive for GFP-DPF coil were defective for endocytosis of MAL and pIgR (Fig. 1 D), whereas they remained competent at internalizing the GPI-anchored FR molecule. Antibody internalization was demonstrated by examining x-z sections of the cells (Fig. 1 A, MAL-FLAG) and by resistance to acid washes (unpublished data). Finally, as a further control, we observed that endocytosis of all MAL-FLAG, pIgR, and FR (unpublished data) was blocked by expression of a dynamin mutant, dyn^{K44A}, defective in GTP binding and hydrolysis (Damke et al., 1994), which impairs both clathrin-dependent and -independent pathways (McNiven et al., 2000).

MAL and pIgR are present in the same apical endocytic vesicles

Because both MAL and pIgR require a functional clathrin-dependent pathway for apical endocytosis, we wondered whether MAL and pIgR are included in the same vesicles during internalization. Keeping in mind that MAL internalizes constitutively without cross-linking with antibodies (Puertollano and Alonso, 1999), to overcome the use of the anti-FLAG antibodies, a construct expressing a MAL protein fused at its amino-terminal end to GFP (GFP-MAL) was used to trace in living cells the movement of MAL from the surface to the cell's interior. The presence of the GFP moiety did affect neither the incorporation of MAL into rafts nor its subcellular distribution (unpublished data). MDCK/pIgR cells grown on coverslips were transiently transfected with GFP-MAL and, after 48 h, cells were incubated with anti-pIgR antibodies coupled to Alexa-594 fluorochrome at 4°C for 30 min. Cells were then shifted to 37°C, and series of images of GFP-MAL and pIgR complexed to the fluorescent anti-pIgR antibodies were analyzed by time-lapse fluorescence confocal microscopy (Fig. 2 and Video 1, available at http://www.jcb.org/cgi/content/full/jcb.200304053/DC1). Within a 5-min period, a significant number of vesicles translocating GFP-MAL and pIgR together from the plasma membrane to the cells's interior were visualized. The GFP-MAL label, which did not emanate from the surface, was distributed in vesicles scattered throughout the cytoplasm and the Golgi complex. Vesicles containing only internalizing pIgR were also identified (unpublished data). The existence of endocytic vesicles with both MAL and pIgR or with pIgR alone in the nonpolarized MDCK cell cultures used are probably reminiscent of the apical and basolateral vesicles, respectively, evidenced in polarized cells. To examine this possibility, we scrutinized the apical and basolateral endocytic vesicles in polarized MDCK cells for the presence of internalized MAL-FLAG and/or pIgR. MDCK cells stably expressing both MAL-FLAG and pIgR (MDCK/MAL-FLAG/pIgR cells) were plated and polarized in culture inserts for 72 h. The apical or the basal side of the cells were incubated with anti-FLAG antibodies coupled to Alexa-488 and with anti-pIgR antibodies coupled to

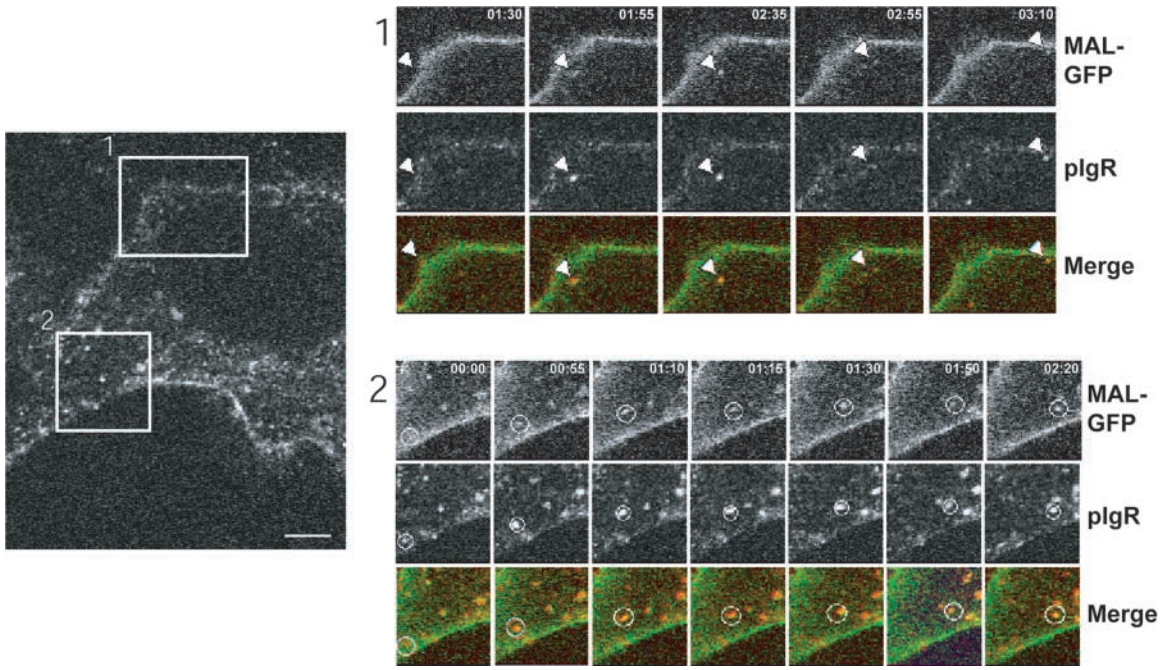

Figure 2. **Time-lapse confocal microscopic analysis of MAL and pIgR internalization.** MDCK/pIgR cells were transiently transfected with GFP-MAL and grown on coverslips. 48 h after transfection, cells were incubated at 4°C for 30 min with antibodies anti-pIgR coupled to Alexa-594, and then shifted to 37°C. Sequential images of GFP-MAL and pIgR bound to the antibody were acquired at 5-s intervals using a confocal fluorescence microscope (see Video 1, available at http://www.jcb.org/cgi/content/full/jcb.200304053/DC1). The left panel shows two membrane regions (1 and 2) selected to illustrate endocytic vesicles in which pIgR and GFP-MAL cointernalization was detected (right panels). Some representative frames obtained in a plane close to the coverslip are shown. The time frame intervals are indicated. The outlined circles and the arrowheads label single vesicles carrying both GFP-MAL and pIgR. Bar, 10 μm.

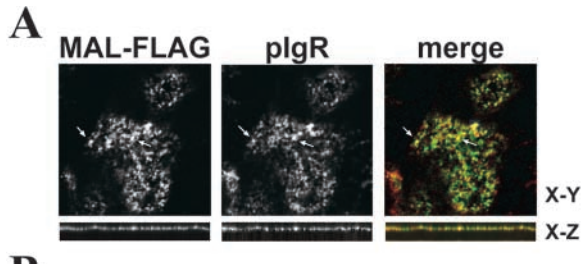

C

	Number of cells analyzed	Total number of vesicles with pIgR	Number of vesicles with pIgR and MAL	%
APICAL	15	540	460	85
BASOLATERAL	12	452	8	1.7

Figure 3. **Double-label confocal analysis of endocytic vesicles in polarized MDCK cells.** MDCK cells stably expressing MAL-FLAG and pIgR were plated onto culture filters and incubated at 37°C for 72 h. Anti-FLAG and anti-pIgR antibodies were coupled to Alexa-488 and Alexa-594, respectively, and applied to the cell monolayers from the apical (A) or the basal (B) side at 4°C for 30 min. Cells were then washed, and shifted at 37°C for 3 min to allow internalization. Cells were fixed and analyzed by confocal microscopy. Images of a (A) subapical x-y plane, an (B) x-y plane corresponding to the contact of the basal surface with the filter, and x-z sections obtained from different fields are shown. Note in the x-z sections that, when the antibodies are added to the apical or basal side, only vesicles in the proximity of the respective cell surface are labeled with no detectable staining in the lateral domains as the antibodies cannot access to them in vivo. Arrows indicate examples of vesicles positively labeled for MAL and pIgR after apical internalization. Bar, 10 μm. (C) Quantitative analysis of pIgR-containing vesicles derived from the apical or the basal surface screened for the simultaneous presence of internalized MAL-FLAG is shown.

Alexa-594 at 4°C for 30 min. After 3 min at 37°C to allow internalization, cells were fixed and analyzed by confocal microscopy. Fig. 3 shows subapical (A) and basal (B) confocal planes of the vesicular structures containing internalized pIgR and/or MAL-FLAG. Quantitative analysis showed that 85% of the apical structures containing internalized pIgR were also positive for MAL-FLAG, whereas fewer than 2% of the vesicles with pIgR internalized from the basal surface were stained for internalized MAL-FLAG (Fig. 3 C).

The presence of pIgR and MAL in the same endocytic structures was further analyzed by cryoimmunoelectron microscopy. MDCK/MAL-FLAG/pIgR cells were incubated sequentially with anti-pIgR antibodies and protein A conjugated to 10-nm-diam gold particles and allowed to internalize the receptor for 3 min at 37°C. Under these conditions, the receptor was observed at the plasma membrane and to a minor extent in endocytic structures (i.e., clathrin-coated and -uncoated pits and vesicles; Fig. 4 A). In this experiment, only the fraction of cells expressing pIgR were labeled, thereby ruling out the possibility of unspecific internalization of protein A–gold. To study the presence of MAL in the endocytic structures labeled for pIgR, ultrathin cryosections were immunolabeled for MAL-FLAG using antitag antibodies. Most of the labeling for MAL was observed in small tubularvesicular elements distributed throughout the cell and at the plasma membrane as described previously (Puertollano et al., 2001). Colocalization of MAL and pIgR was observed at the plasma membrane, pits, and vesicles (Fig. 4, B–E). Some of these pits and vesicles bore a clathrin coat, which was unambiguously identified in cryosections (Fig. 4, A, C, and D) by their characteristic electron-dense appearance and thickness (Martínez-Menárguez et al., 1999, 2001).

MAL depletion blocks apical endocytosis of pIgR but not that of GPI-anchored proteins

The presence of MAL in the apical cell surface, the requirement of a functional clathrin-mediated pathway for internal-

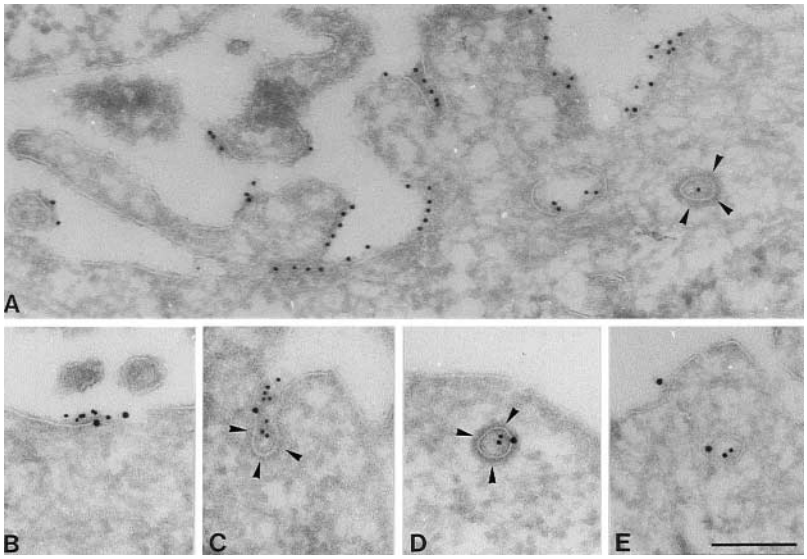

Figure 4. **Colocalization studies of MAL with endocytosed pIgR by immunoelectron microscopy.** (A) MDCK cells expressing MAL-FLAG and pIgR were allowed to internalize the pIgR bound to antibodies and to 10-nm-diam protein A–gold (see Material and methods) for 3 min at 37°C. Analysis of ultrathin cryosection revealed that the receptor–antibody–protein A–gold complex was located at restricted areas of the plasma membrane, pits, and endocytic vesicles. Arrowheads point to a clathrin-coated vesicle containing the internalized receptor complex. (B–E) Ultrathin sections of cells treated as described in A but double immunolabeled for MAL, which is visualized by using antitag antibodies and 15-nm-diam protein A–gold. The micrographs show examples of MAL and pIgR colocalization at the (B) plasma membrane, (C) clathrin-coated pits, (D) clathrin-coated vesicles, and (E) uncoated vesicles. Note the characteristic clathrin coats (arrowheads) in C and D. All micrographs shown were taken at the same magnification. Bar, 200 nm.

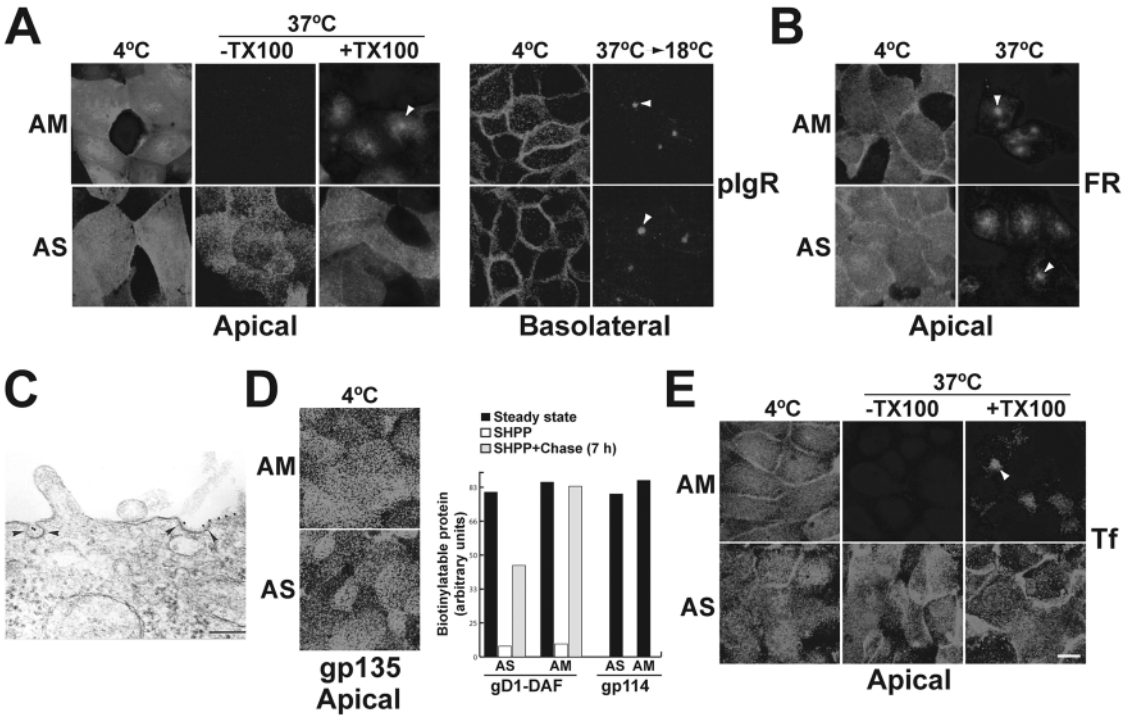

Figure 5. **Effect of MAL depletion on apical endocytosis.** MDCK cells stably expressing (A and C) pIgR, (B) FR, (D) gD1-DAF, or (E) normal cells were transfected with either antisense oligonucleotide AS or control oligonucleotide AM, plated on tissue culture inserts and incubated at 37°C for 48 h. (A) Cells were incubated at either the apical or the basal side with anti-pIgR antibodies for 30 min at 4°C and then at either 4°C or 37°C for 30 min (apical endocytosis) or at either 4°C for 60 min or at 37°C for 10 min followed by incubation at 18°C for 50 min (basolateral endocytosis) to accumulate the pIgR internalized from the basal side in apical endosome compartments (Apodaca et al., 1994). The cells were fixed, permeabilized or not with Triton X-100 (TX100), and incubated with fluorescent secondary antibodies. (B) Cells were incubated at the apical side with anti-FR antibodies coupled to Alexa-594 for 30 min at 4°C. Cells were fixed or incubated at 37°C for 120 min and then fixed and processed for confocal fluorescence microscopy. (C) Cells were incubated at the apical side with anti-pIgR antibodies and protein A coupled to 10-nm-diam gold particles for 30 min at 4°C. After extensive washings, cells were incubated for 30 min at 37°C, fixed and processed for conventional immunoelectron microscopy. Only the result obtained with the cells treated with the oligonucleotide AS is shown. The complex accumulated in clathrin-coated pits with normal morphology (arrowheads). Bar, 200 nm. (D) Cells were incubated at the apical side with anti-gp135 antibodies for 30 min at 4°C and the bound antibody was detected with a fluorescent secondary antibody (left). The apical content of gD1-DAF and gp114 at steady state was determined by labeling with sulfo-NHS-biotin. The new arrival of gD1-DAF at the apical membrane was determined as described in Materials and methods. The intensity of the signals was quantified and is represented in arbitrary units (right). (E) Cells were incubated at the apical side with dog transferrin for 30 min at 4°C. After washing, cells were incubated for 30 min at either 4°C or 37°C to prevent or allow endocytosis, respectively. The cells were then fixed, permeabilized or not with Triton X-100, and sequentially incubated with antitransferrin antibodies and fluorescent secondary antibodies. Bar, 10 mm. In A, B, D, and E, the images shown are of an apical or a basal frame (4°C), to visualize antibody binding, or from a composite projection of all the frames (37°C and 37°C–18°C), to monitor internalization. Endocytosed material is highlighted by arrowheads in A, B, and E.

ization of both MAL and pIgR, and the observed cointernalization of both proteins prompted us to investigate whether MAL is in the vesicles just as a cargo to be recycled or, in addition, plays an active role as machinery for apical internalization of the pIgR. Obviously, MAL internalization is independent of that of pIgR as MAL-FLAG internalizes efficiently in the absence of exogenous pIgR (Fig. 1 A) and MDCK cells lack endogenous expression of this receptor (Breitfeld et al., 1989). To examine the role of MAL in pIgR endocytosis directly, we used specific antisense oligonucleotides to deplete the levels of endogenous MAL as described previously (Puertollano et al., 1999; Martin-Belmonte et al., 2000). Confocal immunofluorescence analysis of MDCK cells polarized in tissue culture inserts shows that depletion of MAL with antisense oligonucleotide AS inhibited apical internalization of pIgR (Fig. 5 A), whereas the internalization of pIgR from the basal surface (Fig. 5 A) or the apical endocytosis of the GPI-anchored proteins FR (Fig. 5 B) and placental alkaline phosphatase (unpublished data) took place at similar levels regardless of the levels of MAL. To investigate the interference of MAL depletion with pIgR internalization at the ultrastructural level, we incubated normal and MAL-depleted MDCK/pIgR cells with anti-pIgR antibodies at 4°C for 20 min followed by protein A–gold. After extensive washing, the cells were incubated for either 2 or 30 min at 37°C to facilitate clustering and pit formation or internalization, respectively. Despite the dramatic effect on pIgR apical internalization seen in MAL-depleted MDCK cells by confocal microscopy (Fig. 5 A), electron microscopic analysis of these cells showed normal receptor clustering and formation of pits with apparent normal morphology and size after 2 min at 37°C (unpublished data). Compared with the apical internalization of the pIgR–antibody complex as assayed by confocal microscopic (Fig. 1 B and Fig. 5 A) or biochemical analyses (see Fig. 6 A), that of the pIgR–antibody–protein A–gold complex was inefficient, such that only ~40% of the complex was in en-

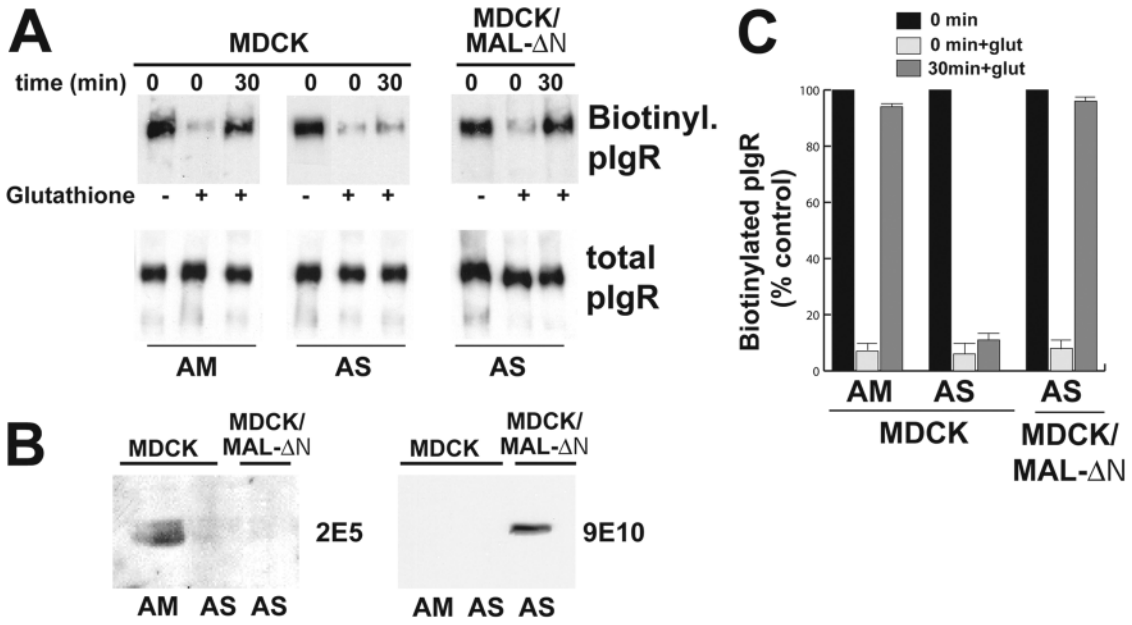

Figure 6. **Biochemical analysis of the effect of MAL depletion on apical endocytosis of the pIgR.** (A) MDCK or MDCK/MAL-ΔN cells stably expressing pIgR were transfected with either antisense oligonucleotide AS or control oligonucleotide AM and plated on tissue culture inserts. After 48 h at 37°C, the apical surface was labeled with NHS-SS-biotin, and the cells were incubated at 4°C or 37°C. After 30 min, the label remaining on the cell surface was removed by glutathione treatment. After immunoprecipitation with specific antibodies, internalized pIgR was visualized by immunoblotting with streptavidin peroxidase. (B) Endogenous MAL levels were quantified by densitometric scanning of the immunoblots of the initial lysates with anti–dog MAL 2E5 mAb (left). As the anti–dog MAL antibody does not react with the human protein (Puertollano et al., 1999), tagged human MAL was detected with antitag antibodies (right). One representative experiment out of six performed is shown. (C) Quantitative analysis of the effect of MAL depletion on apical endocytosis of pIgR. The intensity of the protein bands obtained in the different experiments was quantified by densitometric analysis. The values shown are the mean values expressed as a percentage of the biotinylated pIgR present on the apical surface at 4°C in the absence of glutathione treatment.

docytic compartments after 30 min at 37°C in normal cells. Consistent with the requirement of MAL for efficient apical pIgR endocytosis, in cells with reduced levels of MAL, we observed less internalization and a twofold accumulation of the pIgR–antibody–protein A–gold complex in clathrin-containing pits and vesicles (Fig. 5 C; Table I). Importantly, the ratio between the total number (including structures not labeled with gold particles) of coated pits and coated vesicles at the apical membrane increased from 0.82 in normal cells to 1.44 in MAL-depleted cells. This suggests an impairment in the maturation of the pits to produce vesicles in the cells with reduced levels of MAL.

It is of note that, despite the reduction of MAL levels slowing down delivery of apical cargo through the direct transport route (Cheong et al., 1999; Puertollano et al., 1999; Martin-Belmonte et al., 2000), this treatment did not affect the steady-state levels of the GPI-anchored proteins FR (Fig. 5 B) and gD1-DAF (Lisanti et al., 1989), or the transmembrane gp135 and gp114 apical markers (Fig. 5 D), as analyzed by confocal microscopy (FR and gp135) or selective biotinylation of the apical domain (gD1-DAF and gp114). This leaky transport to the apical surface is probably the result of the remaining MAL molecules being able to deliver cargo, albeit inefficiently, as is shown for gD1-DAF (Fig. 5 D) and was described previously for the influenza virus hemagglutinin (Puertollano et al., 1999). The transferrin receptor uses clathrin for both apical and basolateral internalization (Odorizzi et al., 1996). To determine whether apical internalization of other molecules using clathrin is also dependent on MAL levels, we analyzed the apical endocytosis of iron-loaded transferrin mediated by the endogenous transferrin receptor in MDCK cells (Apodaca et al., 1994). Fig. 5 E shows that whereas transferrin endocytosis took place efficiently in cells transfected with control oligonucleotides AM, most of the transferrin remained at the apical surface in cells whose MAL levels were reduced by treatment with antisense oligonucleotide AS. Transferrin internalization from the basolateral surface was unaffected by the treatment (unpublished data). These results indicate a more general role for MAL in clathrin-mediated apical endocytosis.

To analyze the effect of MAL depletion further, the apical internalization of the pIgR molecule was also investigated by biochemical means (Fig. 6). MDCK/pIgR cells were trans-

Table I. **Distribution of apically internalized pIgR in normal and MAL-depleted MDCK cells**

	Control	MAL-depleted
Plasma membrane excluding coated pits	58.9 ± 3.0	75.9 ± 10.2
Clathrin-coated pits and vesicles	5.0 ± 2.2	11.7 ± 8.0
Rest of endocytic compartments	36.1 ± 5.2	12.4 ± 2.3

Numbers represent the percentages (mean ± SEM) of the pIgR–antibody–protein A–gold complex over the distinct membrane categories. At least 200 gold particles were scored for each type of cell.

fected with either antisense oligonucleotide AS or control oligonucleotide AM and plated in tissue culture inserts. After 48 h at 37°C, the apical surface was labeled at 4°C with sulfosuccinimidyl 2-(6-(biotinamido)hexanoamido)ethyl-1-39-dithiopropionate (NHS-SS-biotin), a reducible analogue of sulfo-*N*-hydroxyl-succinimido-biotin (sulfo-NHS-biotin). Cells were then incubated for 30 min at 37°C to allow internalization and the biotin label that remained on the cell surface was removed by treating the cells with glutathione, leaving the endocytosed label protected from the reducing agent (Lisanti et al., 1990). After immunoprecipitation, internalized pIgR was visualized by immunoblotting with streptavidin peroxidase. An example of the efficiency of the glutathione treatment is shown in the left panel of Fig. 6 A. The vast majority (>90%) of apical pIgR was endocytosed after 30 min in control MDCK cells (Fig. 6 A, top left), whereas only a minor portion (<5%) was internalized (Fig. 6 A, top middle) in cells with whose MAL levels were reduced to ~5% of those in control cells, as quantified by densitometric scanning of the immunoblots obtained with anti-MAL mAb 2E5 (Fig. 6 B). To confirm that these effects were due to MAL depletion and not to spurious effects of the antisense oligonucleotide, we used MDCK/MAL-ΔN cells expressing a truncated form of human MAL (MAL-ΔN) that is resistant to the depletion treatment as its mRNA cannot pair with the antisense oligonucleotide (Fig. 6 B, right; Martin-Belmonte et al., 2000). The exogenous expression of MAL-ΔN allowed normal apical endocytosis of pIgR (Fig. 6 A, right) despite the drop in the amount of endogenous MAL (Fig. 6 B, left). A quantitative analysis of the effect of MAL depletion on apical internalization of pIgR is shown in Fig. 6 C.

Discussion

MAL is essential for efficient endocytosis of the pIgR from the apical surface

Although apical endocytosis is a fundamental process by which polarized epithelia take up soluble molecules, macromolecules and even entire pathogens on the luminal side, its mechanism is still poorly understood. An important feature of the apical membrane is its high raft lipid content (Simons and van Meer, 1988). This makes the apical membrane more rigid compared with the fluid structure of the plasma membrane of nonpolarized cells and the basolateral membrane. The process of clathrin-mediated endocytosis is approximately five times slower at the apical than at the basolateral surface (Naim et al., 1995). Coated pits at the apical surface recognize cargo proteins as efficiently as at the basolateral surface, but their maturation into transport vesicles is much slower. Apparently, the limiting step occurs before the dynamin-directed fission of the vesicle takes place. To explain this difference the existence was proposed of an apical membrane factor that either controls the addition of clathrin triskelions into the lattice or regulates membrane curvature (Naim et al., 1995). Consistent with the reported presence of MAL in clathrin-coated pits (Puertollano et al., 2001), herein we show that MAL endocytosis is blocked by expression of a dominant negative Eps15 mutant known to interfere specifically with clathrin-mediated endocytosis, such as apical internalization of pIgR. In addition to having the same requirements, the cotransport of pIgR and MAL observed in living cells by time-lapse confocal immunofluorescence analysis and the presence of internalized pIgR in MAL-containing pits and vesicles as revealed by electron microscopic analysis were consistent with a possible role for MAL in apical endocytosis of the pIgR. The involvement of MAL in this process was demonstrated by the block of pIgR internalization observed in the apical surface, but not in the basolateral, in cells in which the levels of MAL were reduced by treatment with specific antisense oligonucleotides. It is of note that the apical endocytosis of GPI-anchored proteins FR and placental alkaline phosphatase were unaffected by MAL depletion, whereas internalization of the transferrin receptor from the apical surface, a process known to require clathrin (Odorizzi et al., 1996), was also dependent on normal MAL levels. This is consistent with the fact that apical internalization of GPI-anchored protein occurs by a different pathway that does not involve clathrin and that, in contrast to apical internalization of pIgR and transferrin receptor, which requires MAL and clathrin, appears to use caveolin-1 as the machinery for the formation of endocytic pits and intracellular transport vesicles resembling caveolae (Verkade et al., 2000).

A direct role or a secondary effect?

The reduction of MAL content slows down the delivery of apical cargo but apical transport is not completely ablated, probably because of the remaining MAL molecules (Puertollano et al., 1999; Martin-Belmonte et al., 2000). As a consequence of this "leaky" transport, the steady-state content of apical proteins is similar in both normal and MAL-depleted MDCK cells (Martin-Belmonte et al., 2000). Consistent with this, we observed similar levels of FR, placental alkaline phosphatase, gD1-DAF, gp135, and gp114 in the apical membrane regardless of the levels of MAL, although we have previously shown that GPI-anchored cargo proteins and transmembrane proteins require MAL for efficient apical transport (Martin-Belmonte et al., 2000). Therefore, although it cannot be ruled out, it is unlikely that MAL depletion reduces specifically the steady-state apical levels of a hypothetical cargo molecule important for apical endocytosis of pIgR but not for that of GPI-anchored proteins. The simplest explanation for all our observations is that the reduction of the MAL content directly affects apical internalization of pIgR.

MAL as machinery for the formation of clathrin-coated apical endocytic vesicles

The observations that (1) MAL is required for apical transport (Cheong et al., 1999; Puertollano et al., 1999; Martin-Belmonte et al., 2000); (2) apical cargo accumulates in the Golgi complex in MDCK cells with reduced levels of MAL (Cheong et al., 1999; Martin-Belmonte et al., 2001); and (3) overexpression of MAL results in de novo formation of a large number of intracellular vesicles (Puertollano et al., 1997), led to the proposal that MAL is an element of the machinery involved in the formation of apical transport vesicles. We have not observed significant differences in the initial processes of pIgR clustering and formation of coated pits at

the apical surface between normal MDCK cells and cells with reduced levels of MAL, although an accumulation of the pIgR in clathrin pits and buds was observed at later times in MAL-depleted cells, which is consistent with apical internalization of the pIgR being blocked by MAL depletion. We have recently demonstrated that MAL2, a novel raft protein of the MAL family (Perez et al., 1997), is essential for the exit of vesicular carriers from perinuclear endosomes so that they may travel to the apical membrane during transcytotic transport in hepatoma HepG2 cells (de Marco et al., 2002). It has been proposed that synaptophysin, a tetraspan protein of the physin family, participates in the biogenesis of the synaptic vesicles (Thiele et al., 2000; Huttner and Zimmerberg, 2001). It is of note that MAL family proteins share a protein sequence motif, referred to as the MARVEL motif, with physins and gyrins that it is thought to play a role in membrane trafficking (Sánchez-Pulido et al., 2002). Therefore, we find it plausible that MAL, the other members of the MAL family, and probably other proteins containing a MARVEL domain could serve as machinery for lipid remodelling during biogenesis of transport vesicles. Consistent with this, our present results indicate that MAL is essential for the process of clathrin-mediated internalization of the pIgR in the raft-enriched apical surface and that the maturation process of apical-coated pits to produce vesicles appears to be impaired in cells with reduced levels of MAL.

Materials and methods

Materials

The mouse hybridoma that produces mAb 9E10 to the c-Myc epitope was purchased from the American Type Culture Collection. Rabbit polyclonal antibodies to pIgR were purchased from DakoCytomation (Glostrup). Peroxidase-conjugated anti–mouse or anti–rabbit IgG antibodies, peroxidase-coupled streptavidin, NHS-SS-biotin, sulfo-*N*-hydroxyl-succinimido-phenyl-propionate, and sulfo-NHS-biotin were purchased from Pierce Chemical Co. Fluorochrome-conjugated secondary antibodies were purchased from Southern Biotechnology Associates, Inc. The Alexa fluor–488 and –594 antibody labeling kits were from Molecular Probes. The anti–human FR antibodies and the human FR cDNA construct were donations from L. Kremer (Centro Nacional de Biotecnología, Madrid, Spain); the antibodies to the gp135 and gp114 apical markers were gifts from E. Rodriguez-Boulan (Cornell University, New York, NY). The anti–dog transferrin antibodies were donated by K. Mostov (University of San Francisco, San Francisco, CA). Anti-FLAG M2 antibodies and dog transferrin were obtained from Sigma-Aldrich. Protein A–gold was obtained from the Department of Cell Biology at Utrecht University.

Cell culture conditions, transfections, and DNA constructs

Epithelial MDCK II cells were grown on Petri dishes, glass coverslips, or tissue culture inserts in DME supplemented with 10% FBS (Sigma-Aldrich), 50 units/ml penicillin, and 50 μg/ml streptomycin, at 37°C in an atmosphere of 5% CO_2/95% air.

The MAL-FLAG construct, encoding MAL modified at its last extracellular loop by insertion of the sequence DYKDDDDK, which contains the FLAG epitope (DYKD), and the construct expressing a human MAL protein lacking the four amino acids contiguous with the initial methionine residue and bearing the 9E10 c-Myc epitope (MAL-ΔN) have been described previously (Puertollano and Alonso, 1999; Martin-Belmonte et al., 2000). The construct expressing MAL fused at its amino terminus to GFP (GFP-MAL) was generated by cloning a DNA fragment with the MAL coding sequence, except the ATG translation initiation site, in-frame with the last codon of the GFP coding sequence contained in the pEGFP-C1 DNA vector (BD Biosciences). Transfections were done by electroporation using an electroporation instrument (model ECM 600; BTX). Selection of stable MDCK cell transfectants was performed by treatment with either 0.5 mg/ml G418 sulfate (Sigma-Aldrich), or 0.5 μg/ml puromycin (Sigma-Aldrich) for 4 wk after transfection. Drug-resistant clones were picked up with cloning rings, and individual clones were screened by immunofluorescence analysis with the appropriate antibodies. The clones that proved to be positive were maintained in drug-free medium. After several passages through this medium, ~60–70% of cells within the selected positive clones retained expression of the exogenous product. The 19-mer phosphorothioate oligonucleotide AS, complementary to canine MAL mRNA, and the oligonucleotide control AM, similar in composition to AS but with some replacements to prevent pairing with endogenous MAL mRNA, have been described previously (Puertollano et al., 1999; Martin-Belmonte et al., 2000). The GFP-DPF coil DNA construct, the EH deleted form of the Eps15 protein coupled to GFP was a gift of A. Sorkin (University of Colorado, Denver, CO).

Domain-selective labeling with biotin-containing reagents

For separate access to apical or basolateral domains, MDCK cells were seeded at confluent levels on 24-mm polyester tissue culture inserts of 0.4 μm pore size (Transwell; Costar Inc.). The integrity of the cell monolayer was monitored by measuring the transepithelial electrical resistance using the Millicell ERS apparatus (Millipore). To follow the endocytosis of pIgR and FR, we used the protocol described previously by Lisanti et al. (1990). In brief, 0.5 mg/ml NHS-SS-biotin was added either to the apical or basolateral compartment of the filter chamber. After 30 min at 4°C, the solution was removed and remaining unreacted biotin quenched by incubation with ice cold serum-free culture medium. Cells were then incubated at 37°C in prewarmed normal medium to allow endocytosis. At the indicated times, the biotin label remaining on the cell surface was stripped by reduction with two sequential treatments with 50 mM glutathione at 4°C. Cell monolayers were extensively washed and extracted with 0.5 ml of 25 mM Tris-HCl, pH 7.5, 150 mM NaCl, 5 mM EDTA, 1% Triton X-100, and 60 mM octyl-glucoside for 30 min on ice. Extracts were immunoprecipitated, and fractionated by SDS-PAGE. Biotinylated proteins were detected by immunoblotting with streptavidin peroxidase.

The steady-state levels of gD1-DAF and gp114 at the apical surface of MDCK cells stably expressing exogenous gD1-DAF were determined by labeling the apical surface with 0.5 mg/ml sulfo-NHS-biotin. To determine the delivery of gD1-DAF to the apical surface, cells were pretreated at the apical compartment with 0.5 mg/ml sulfo-*N*-hydroxyl-succinimido-phenyl-propionate, which lacks the biotin moiety, for 10 min to quench free amino groups. The solution was removed and the treatment was repeated five times to quench residual free amino groups (Lisanti et al., 1990). After incubation for 7 h at 37°C, the appearance of newly delivered molecules on the cell surface was monitored by domain-selective labeling with sulfo-NHS-biotin. Finally, lysates were subjected to immunoprecipitation with the appropriate antibody coupled to protein G–Sepharose, and immunoblotting with streptavidin peroxidase. Using this procedure, it was determined previously that 95% of the newly arrived population of gD1-DAF is due to biosynthetic delivery, whereas the remaining 5% may represent a recycling pool (Lisanti et al., 1990).

Immunoprecipitation and immunoblot analyses

For use in immunoprecipitation studies, antibodies were prebound overnight to protein G–Sepharose in 10 mM Tris-HCl, pH 8.0, 0.15 M NaCl, and 1% Triton X-100 at 4°C. Postnuclear supernatants, prepared with 1% Triton X-100 plus 60 mM octyl-glucoside, were incubated at 4°C for 4 h with a control antibody bound to protein G–Sepharose. After centrifugation, the supernatant was immunoprecipitated by incubation 4°C for 4 h with the appropriate antibody bound to protein G–Sepharose. The immunoprecipitates were collected, washed six times with 1 ml of 10 mM Tris-HCl, pH 8.0, 0.15 M NaCl, and 1% Triton X-100, and fractionated by SDS-PAGE. For immunoblot analysis, samples were transferred to Immobilon-P membranes (Millipore) and blocked with 5% nonfat dry milk and 0.05% Tween 20 in PBS. The blots were then incubated with the indicated primary antibody. After several washings, blots were incubated for 1 h with secondary anti-IgG antibodies coupled to HRP, washed extensively, and developed using an ECL Western blotting kit (Amersham Biosciences).

Immunofluorescence and time-lapse confocal microscopic analyses

For immunofluorescence microscopy, cells grown on culture filters or on coverslips were washed twice with PBS, fixed in 4% PFA for 15 min, rinsed, and treated with 10 mM glycine for 10 min to quench the aldehyde groups. Then, cells were permeabilized or not with 0.2% Triton X-100 and were incubated with 3% BSA for 20 min. After incubation with the appropriate primary and secondary antibodies, images were obtained using a confocal laser microscope (model radiance 2000; Bio-Rad Laboratories) or a conventional fluorescence microscope (Carl Zeiss MicroImagining, Inc.). In

some of the experiments presented here, a specific fluorescent primary antibody was used in living cells to monitor internalization and the cells were processed for immunofluorescence analysis directly after fixation. For time-lapse confocal fluorescence microscopy, MDCK cells expressing GFP-MAL and pIgR grown on coverslips were incubated with anti-pIgR antibodies coupled to Alexa-594 for 30 min at 4°C, washed, and incubated at 37°C in a thermal-controlled chamber coupled to the confocal microscope. GFP-MAL and pIgR images were transferred to a computer workstation running MetaMorph imaging software (Universal Imaging Corp.). Cells images were captured at 5-s intervals using a 63× lens. Controls to assess the specificity and the lack of cross-labeling, included incubations with control primary antibodies or omission of either of the primary antibodies.

Immunoelectron microscopy

MDCK/MAL-FLAG/pIgR cells grown on culture filters were incubated at the apical side with anti-pIgR antibodies followed by protein A coupled to 10-nm gold particles, extensively washed and incubated at 37°C for 3 min. Thereafter, the cells were fixed 2 h with 2% PFA and 0.2% glutaraldehyde in 0.1 M phosphate buffer, removed from the filters, and processed for cryosectioning as described previously (Martínez-Menárguez et al., 1999, 2001). In brief, the cells were collected by centrifugation, embedded in 10% gelatin, and cut into small blocks. The blocks were infused overnight with 2.3 M sucrose, mounted in aluminum pins, frozen in liquid nitrogen, and stored until cryoultramicrotomy. Ultrathin cryosections were immunolabeled with antitag antibody followed by a bridging rabbit anti–mouse IgG antibody and protein A coupled to 15-nm gold particles. For conventional electron microscopic studies, normal or MAL-depleted cells grown on culture filters were incubated at the apical side with anti-pIgR antibodies followed by protein A coupled to 10-nm gold particles, extensively washed and incubated for either 2 or 30 min at 37°C. Cells were then fixed for 2 h with 2% PFA and 0.2% glutaraldehyde, fixed after for 2 h with 1% osmium, and embedded in Epon using standard techniques. To quantify the relative distribution of the internalized pIgR–antibody–protein A–gold complex, ultrathin sections of Epon-embedded normal and MAL-depleted MDCK cell monolayers were scanned directly along their apical portion under the electron microscope at a magnification of 20,000. Gold particles ($n > 200$) were ascribed to one of the after categories: plasma membrane (excluding coated pits), clathrin-coated pits and vesicles, and the rest of endocytic membranes (noncoated vesicles and endosomes). The number of gold particles found over each compartment was expressed as percentage of the total number of particles scored (Table I). In addition, cells from the same experiment were scanned along their apical area to measure the ratio between clathrin-coated pits and clathrin-coated vesicles. This was done directly from the screen of the microscope working at a magnification of 30,000. Only coated structures found on the apical membrane or in the cytoplasm within a distance of 300 nm from the apical membrane (approximately threefold the typical thickness of a coated vesicle) were considered. A total number of 100 coated structures (labeled or not) from fields randomly sampled were scored, and the ratio between pits and vesicles was calculated in normal and MAL-depleted MDCK cells.

Online supplemental material

Video 1 accompanies Fig. 2 and shows two examples of cointernalization of pIgR–antibody complexes (red) and MAL-GFP (green) in MDCK cells. Frames were collected every 5 s. The display rate is 9.5 frames/s. Online supplemental material is available at http://www.jcb.org/cgi/content/full/jcb.200304053/DC1.

We thank S. Gómez and C. Sánchez for technical help.

This work was supported by grants from the Comunidad de Madrid (08.5/0066/2001.1), Ministerio de Ciencia y Tecnología (PM99-0092 and BMC2003-03297), Fondo de Investigación Sanitaria (01/0085-01), and Fundación Eugenio Rodríguez Pascual to M.A. Alonso; from Ministerio de Ciencia y Tecnología (PM99-0137 and BFI2000-0156) to J. Ballesta; and Fundación Séneca (PB/49/FS/02) to J.A. Martínez-Menárguez. An institutional support from Fundación Ramón Areces is also acknowledged.

Submitted: 10 April 2003
Accepted: 14 August 2003

References

Altschuler, Y., S. Liu, L. Katz, K. Tang, S. Hardy, F. Brodsky, G. Apodaca, and K. Mostov. 1999. ADP-ribosylation factor 6 and endocytosis at the apical surface of Madin-Darby canine kidney cells. *J. Cell Biol.* 147:7–12.

Apodaca, G., L.A. Katz, and K.E. Mostov. 1994. Receptor-mediated transcytosis of IgA in MDCK cells is via apical recycling endosomes. *J. Cell Biol.* 125:67–86.

Benmerah, A., M. Bayrou, N. Cerf-Bensussan, and A. Dautry-Varsat. 1999. Inhibition of clathrin-coated pit assembly by an Eps15 mutant. *J. Cell Sci.* 112: 1303–1311.

Breitfeld, P.P., J.M. Harris, and K.E. Mostov. 1989. Postendocytic sorting of the ligand for the polymeric immunoglobulin receptor in Madin-Darby canine kidney cells. *J. Cell Biol.* 109:475–486.

Cheong, K.H., D. Zacchetti, E.E. Schneeberger, and K. Simons. 1999. VIP17/MAL, a lipid raft-associated protein, is involved in apical transport in MDCK cells. *Proc. Natl. Acad. Sci. USA.* 96:6241–6248.

Damke, H., T. Baba, D.E. Warnock, and S.L. Schmid. 1994. Induction of mutant dynamin specifically blocks endocytic coated vesicle formation. *J. Cell Biol.* 127:915–934.

de Marco, M.C., F. Martín-Belmonte, L. Kramer, J.P. Albar, I. Correas, J.P. Vaerman, M. Marazuela, J.A. Byrne, and M.A. Alonso. 2002. MAL2, a novel raft protein of the MAL family, is an essential component of the machinery for transcytosis. *J. Cell Biol.* 159:37–44.

Huttner, W.B., and J. Zimmerberg. 2001. Implications of lipid microdomains for membrane curvature, budding and fission. *Curr. Opin. Cell Biol.* 13:478–484.

Lisanti, M.P., I.W. Caras, M.A. Davitz, and E. Rodriguez-Boulan. 1989. A glycophospholipid membrane anchor acts as an apical targeting signal in polarized epithelial cells. *J. Cell Biol.* 109:2145–2156.

Lisanti, M.P., I.W. Caras, T. Gilbert, D. Hanzel, and E. Rodriguez-Boulan. 1990. Vectorial apical delivery and slow endocytosis of a glycolipid-anchored fusion protein in transfected MDCK cells. *Proc. Natl. Acad. Sci. USA.* 87: 7419–7423.

Martin-Belmonte, F., R. Puertollano, J. Millan, and M.A. Alonso. 2000. The MAL proteolipid is necessary for the overall apical delivery of membrane proteins in the polarized epithelial Madin-Darby canine kidney and Fischer rat thyroid cell lines. *Mol. Biol. Cell.* 11:2033–2045.

Martin-Belmonte, F., P. Arvan, and M.A. Alonso. 2001. MAL mediates apical transport of secretory proteins in polarized epithelial Madin-Darby canine kidney cells. *J. Biol. Chem.* 276:49337–49342.

Martínez-Menárguez, J.A., H.J. Geuze, J.W. Slot, and J. Klumperman. 1999. Vesicular tubular clusters between the ER and the Golgi mediate concentration of soluble secretory proteins by exclusion from COPI-coated vesicles. *Cell.* 98:81–90.

Martínez-Menárguez, J.A., R. Prekeris, V.M. Oorshot, R. Scheller, H.J. Geuze, J.W. Slot, and J. Klumperman. 2001. Peri-Golgi vesicles contain retrograde but not anterograde proteins consistent with the cisternal-progression model of intra-Golgi transport. *J. Cell Biol.* 155:1213–1224.

Matter, K., and I. Mellman. 1994. Mechanisms of cell polarity: sorting and transport in epithelial cells. *Curr. Opin. Cell Biol.* 6:545–554.

McNiven, M.A., H. Cao, K.R. Pitts, and Y. Yoon. 2000. The dynamin family of mechanoenzymes: pinching in new places. *Trends Biochem. Sci.* 25:115–120.

Mellman, I., E. Yamamoto, J.A. Whitney, M. Kim, W. Hunzinker, and K. Matter. 1993. Molecular sorting in polarized and non-polarized cells: common problems, common solutions. *J. Cell Sci. Suppl.* 17:1–7.

Mostov, K.E., M. Verges, and Y. Altschuler. 2000. Membrane traffic in polarized epithelial cells. *Curr. Opin. Cell Biol.* 12:483–490.

Naim, H.Y., D.T. Dodds, C.B. Brewer, and M.G. Roth. 1995. Apical- and basolateral-coated pits of MDCK cells differ in their rates of maturation into coated vesicles, but not in the ability to distinguish between mutant hemagglutinin proteins with different internalization signals. *J. Cell Biol.* 129: 1241–1250.

Nichols, B.J., and J. Lippincott-Schwartz. 2001. Endocytosis without clathrin coats. *Trends Cell Biol.* 11:406–412.

Odorizzi, G., A. Pearse, D. Domingo, I.S. Trowbridge, and C.R. Hopkins. 1996. Apical and basolateral endosomes of MDCK cells are interconnected and contain a polarized sorting mechanism. *J. Cell Biol.* 135:139–152.

Perez, P., R. Puertollano, and M.A. Alonso. 1997. Structural and biochemical similarities reveal a family of proteins related to the MAL proteolipid, a component of detergent-insoluble membrane microdomains. *Biochem. Biophys. Res. Commun.* 232:618–621.

Puertollano, R., and M.A. Alonso. 1999. MAL, an integral element of the apical sorting machinery, is an itinerant protein that cycles between the trans-Golgi network and the plasma membrane. *Mol. Biol. Cell.* 10:3435–3447.

Puertollano, R., S. Li, M.P. Lisanti, and M.A. Alonso. 1997. Recombinant expression of the MAL proteolipid, a component of glycolipid-enriched membrane

microdomains, induces the formation of vesicular structures in insect cells. *J. Biol. Chem.* 272:18311–18315.

Puertollano, R., F. Martin-Belmonte, J. Millan, M.C. de Marco, J.P. Albar, L. Kremer, and M.A. Alonso. 1999. The MAL proteolipid is necessary for normal apical transport and accurate sorting of the influenza virus hemagglutinin in Madin-Darby canine kidney cells. *J. Cell Biol.* 145:141–151.

Puertollano, R., J.A. Martínez-Menárguez, A. Batista, J. Ballesta, and M.A. Alonso. 2001. An intact dilysine-like motif in the carboxyl terminus of MAL is required for normal apical transport of the influenza virus hemagglutinin cargo protein in epithelial Madin-Darby canine kidney cells. *Mol. Biol. Cell.* 12:1869–1883.

Sánchez-Pulido, L., F. Martín-Belmonte, A. Valencia, and M.A. Alonso. 2002. MARVEL: a conserved domain involved in membrane apposition events. *Trends Biochem. Sci.* 27:599–601.

Simons, K., and G. van Meer. 1988. Lipid sorting in epithelial cells. *Biochemistry.* 27:6197–6202.

Simons, K., and A. Wandinger-Ness. 1990. Polarized sorting in epithelia. *Cell.* 62: 207–210.

Thiele, C., M.J. Hannah, F. Fahrenholz, and W.B. Huttner. 2000. Cholesterol binds to synaptophysin and is required for biogenesis of synaptic vesicles. *Nat. Cell Biol.* 2:42–49.

Verkade, P., T. Harder, F. Lafont, and K. Simons. 2000. Induction of caveolae in the apical membrane of Madin-Darby canine kidney cells. *J. Cell Biol.* 148: 727–739.